

## Plasma-Wakefield Acceleration of an Intense Positron Beam

B. E. Blue,<sup>1</sup> C. E. Clayton,<sup>1</sup> C. L. O'Connell,<sup>2</sup> F.-J. Decker,<sup>2</sup> M. J. Hogan,<sup>2</sup> C. Huang,<sup>1</sup> R. Iverson,<sup>2</sup> C. Joshi,<sup>1</sup>  
T. C. Katsouleas,<sup>3</sup> W. Lu,<sup>1</sup> K. A. Marsh,<sup>1</sup> W. B. Mori,<sup>1</sup> P. Muggli,<sup>3</sup> R. Siemann,<sup>2</sup> and D. Walz<sup>2</sup>

<sup>1</sup>University of California, Los Angeles, California 90095, USA

<sup>2</sup>Stanford Linear Accelerator Center, Stanford, California 94309, USA

<sup>3</sup>University of Southern California, Los Angeles, California 90089, USA

(Received 15 February 2003; published 30 May 2003)

Plasma wakefields are both excited and probed by propagating an intense 28.5 GeV positron beam through a 1.4 m long lithium plasma. The main body of the beam loses energy in exciting this wakefield while positrons in the back of the same beam can be accelerated by the same wakefield as it changes sign. The scaling of energy loss with plasma density as well as the energy gain seen at the highest plasma density is in excellent agreement with simulations.

DOI: 10.1103/PhysRevLett.90.214801

PACS numbers: 41.75.Ht, 41.75.Lx, 52.40.Mj

High-gradient acceleration of both positrons and electrons is a prerequisite condition to the successful development of a plasma-based  $e^+e^-$  linear collider. Such an accelerator employs the longitudinal electric field of a relativistically propagating wakefield in a plasma to accelerate charged particles [1–3]. In proof-of-principle experiments, laser-driven plasma wakefields have been shown to accelerate electrons at gradients that are significantly greater than those employed in current radio-frequency accelerators [4–7]. In this Letter we show for the first time that a beam of positrons can drive and be used to probe the longitudinal electric field component of the plasma wakefield. When a 28.5 GeV, 2.4 ps long positron beam at the Stanford Linear Accelerator Center (SLAC) containing  $1.2 \times 10^{10}$  particles propagates through a lithium plasma of electron density  $1.8 \times 10^{14} \text{ cm}^{-3}$ , the main body of the beam is decelerated at a rate of approximately 49 MeV/m, while a beam slice containing  $5 \times 10^8$  positrons in the back of the same bunch gains energy at an average rate of  $\sim 56$  MeV/m over 1.4 m. These results are critical to the development of future plasma-based linear colliders.

When an ultrarelativistic, highly focused ( $\sigma_r \ll c/\omega_p$ ) positron beam enters an underdense plasma ( $n_b > n_p$ ), the in-vacuum balance between the beam's space-charge defocusing field and self-magnetic focusing field is modified by the highly mobile plasma electrons that are pulled in neutralizing the excess space charge of the positron beam. Here  $\sigma_r$ ,  $c$ ,  $\omega_p$ ,  $n_b$ , and  $n_p$  are the beam radius, speed of light, plasma frequency, beam density, and plasma density, respectively. The degree of neutralization depends not only on the plasma density but also on the longitudinal position along the positron bunch. This in turn leads to a longitudinal and transverse nonuniform focusing force that nevertheless can focus the beam [8,9]. While the focusing of the positron beam by the transverse fields has been experimentally demonstrated, there has not been a systematic investigation of the longitudinal component of the wakefield induced by the positron beam

in a plasma. As plasma electrons from various radii arrive on the axis of the beam at various times and overshoot, they create a wakefield structure that has complex longitudinal and transverse electric field components [10]. In this experiment, a single positron bunch is used to both excite and probe the longitudinal electric field component of the plasma wakefield with picosecond resolution by diagnosing the energy change of different longitudinal slices of the drive beam itself. If the rms bunch length  $\sigma_z$  is approximately  $\pi c/\omega_p$ , then the bulk of the positrons do work in pulling in the plasma electrons and therefore lose energy to the wakefield. However, there are a significant number of particles in the latter half of the beam where the wakefield has changed sign and are therefore accelerated. For instance, Fig. 1 shows the plasma wakefield (red curve) induced by a 28.5 GeV positron beam with  $\sigma_z/c = 2.4$  ps, containing  $1.2 \times 10^{10}$  positrons (dashed blue curve) in a  $1.8 \times 10^{14} \text{ cm}^{-3}$  plasma obtained using the 3D, particle-in-cell (PIC) code OSIRIS [11]. The bunch is moving from right to left with the head, or front of the beam, located  $\sim 7$  ps ahead of the centroid, and the tail, or back of the bunch, located  $\sim 7$  ps behind the centroid. The simulation parameters consisted of grid sizes  $\Delta x = \Delta y = \Delta z = 50 \text{ }\mu\text{m}$ , eight plasma particles per cell, 12 beam particles per cell, and a moving simulation window of  $3.2 \text{ cm} \times 3.2 \text{ cm} \times 6.4 \text{ cm}$  in  $x$ ,  $y$ , and  $z$ , respectively. The  $E_z$  field was averaged over  $0 \leq r \leq \sigma_r$  in the simulation grid. Near the beam center (centroid), the peak decelerating field  $E_z^-$  is approximately 50 MV/m, whereas the peak accelerating field  $E_z^+$  located 3 ps after the centroid is approximately 64 MV/m. With such a field structure, the beam energy is transferred from a large number of particles in the core of the bunch to a fewer number of particles in the back of the same bunch. The wakefield thus acts like a transformer with a ratio  $E_z^+/E_z^-$  of  $\sim 1.3$ . Figure 2 shows the predicted change in beam energy vs position in the beam after propagating through 1.4 m of  $1.8 \times 10^{14} \text{ cm}^{-3}$  plasma obtained from the same 3D PIC simulation used to generate the fields of

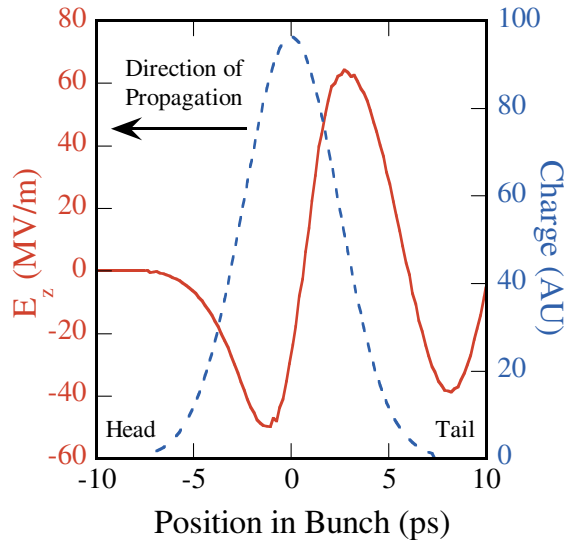


FIG. 1 (color). Longitudinal electric field (solid red curve) excited in a plasma by a positron beam which is moving right to left in the figure (dashed blue curve). The field is averaged over one  $\sigma_z$ . A peak decelerating field of 50 MV/m occurs 1 ps ahead of the centroid and a peak accelerating field of 64 MV/m occurs 3 ps behind the centroid.

Fig. 1. The beam is traveling from right to left with the head and tail marking the front and back of the beam, respectively. The color-mapped intensity at each point in the graph is proportional to the number of beam particles within a  $\Delta\text{energy} \times \Delta\text{time}$  grid point. The peak energy loss of the beam is about 64 MeV, whereas the “slice” of the bunch located  $\sim 1.7\sigma_z$  behind the peak energy loss location (i.e., the slice at 3 ps) has gained approximately 80 MeV. The maximum energy gain and loss seen in the

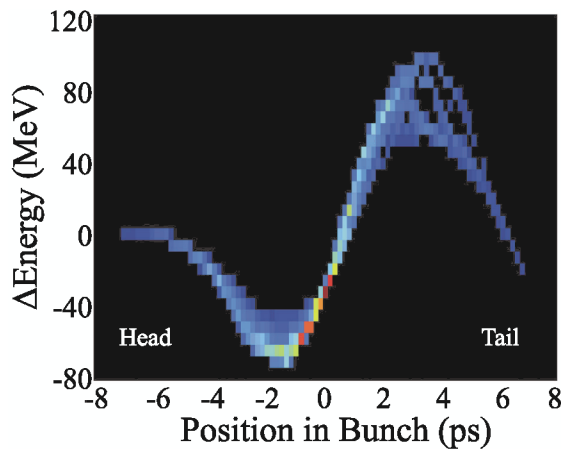


FIG. 2 (color). 3D particle-in-cell simulation of a positron beam in a plasma. The image depicts the phase space of the beam after it has traversed 1.4 m of plasma. Beam parameters in the simulation were identical to experimental parameters. The simulation predicts an energy loss of 64 MeV and an energy gain of 79 MeV.

OSIRIS simulations are consistent with the transformer ratio inferred from the plot of the longitudinal field of Fig. 1 demonstrating that once established, the longitudinal fields do not significantly evolve as the beam propagates through the plasma.

The experiment took place in the Final Focus Test Beam facility at the SLAC. A 28.5 GeV positron beam with  $N = 1.2 \times 10^{10}$  particles ( $\sim 1.9$  nC) in a  $\sigma_z = 0.73$  mm long bunch was focused at the plasma entrance with a spot size of  $\sigma_r = 40 \mu\text{m}$ . The beam’s charge was measured using current monitors before and after the plasma, the incoming spot size was measured by imaging the optical transition radiation emitted by the positron beam passing through a  $37 \mu\text{m}$  thick titanium foil onto a charge coupled device (CCD) camera [12], and the incoming beam energy before entering the plasma was monitored using a beam position monitor in a dispersive section of the beam line upstream of the plasma. The plasma source [13] consisted of an ionized lithium vapor (ionization potential = 5.4 eV) in a heat pipe oven which had a neutral gas density of  $N_g = 2 \times 10^{15} \text{cm}^{-3}$  over a length of 1.4 m. The plasma was created via single photon ionization of lithium atoms using a pulse from a 193 nm (photon energy = 6.4 eV) argon fluoride excimer laser. The plasma density was varied between  $0\text{--}2 \times 10^{14} \text{cm}^{-3}$  by varying the laser pulse energy. The laser pulse energy was measured before and after the lithium vapor column on every shot, and therefore the plasma density was known for every shot.

Upon exiting the plasma, the positron beam was imaged with a magnetic imaging spectrometer with a magnification of 3 in both the horizontal and vertical planes onto a 1 mm thick aerogel Cherenkov radiator located 25 m away [1]. The magnetic dispersion of 291 MeV/mm at the Cherenkov radiator spread the beam out in the vertical plane, so that by measuring the vertical position of different longitudinal slices of the beam at the Cherenkov plane, the beam energy distribution could be determined. Since the vertical displacement at the aerogel induced by the energy changes of the beam in the plasma was on the order of the beam’s spot size, time resolution of the beam was necessary to separate the energy changes of the beam’s various longitudinal slices. The Cherenkov radiation was imaged onto both a CCD camera for a time-integrated energy diagnostic and onto the slit of a streak camera with 1 ps temporal resolution for time-resolved measurements. The time-integrated energy diagnostic was used to monitor the positron beam’s transverse shape and to determine which portion of the beam was sampled by the streak camera slit. The Cherenkov radiation which was sent to the streak camera was first split into two paths with a beam splitter. One arm was passed through a  $90^\circ$  rotator and a time delay before it was recombined with the other arm to produce two orthogonal images ( $y$  vs  $t$  and  $x$  vs  $t$ ) on the streak camera. The vertical streak camera image ( $y$  vs  $t$ ) thus measured the

temporal energy variation of the positron beam while the horizontal streak camera image ( $x$  vs  $t$ ) measured the transverse (dispersion-free) dynamics.

A primary indicator that the positron beam is driving, and thus transferring energy to, a plasma wakefield is the observation of energy loss. Energy loss measurements over a wide range of plasma densities are presented in Fig. 3 (blue circles). Figure 3 also shows the energy loss predictions from 3D PIC simulations (red triangles). The energy loss of the beam was measured after the plasma by dividing the entire energy-dispersed streak camera image into 1 ps slices, fitting a Gaussian profile to the data of each slice and tracking the relative position of each Gaussian's mean. The plasma density was varied between  $0$ – $2 \times 10^{14} \text{ cm}^{-3}$  over a series of 200 shots. The ionizing laser was not fired every fourth shot to provide a baseline measurement of incoming beam parameters and to provide the data for zero plasma density. The measured mean positions were binned by plasma density, and the peak energy loss was calculated for each density by subtracting the mean of the incoming beam energy from the mean of the slice which lost the greatest energy after the plasma. The vertical error bars represent the standard deviation of the mean for each density bin. As can be seen in Fig. 3, simulations predict and experimental data confirm that the beam loses energy in the plasma. The energy loss gradually increases with increasing plasma density with a maximum measured energy loss of  $68 \pm 8 \text{ MeV}$  at a plasma density of  $1.8 \times 10^{14} \text{ cm}^{-3}$ . This is in good agreement with 3D OSIRIS simulations which predicted a peak energy loss of  $64 \text{ MeV}$  at the same plasma density.

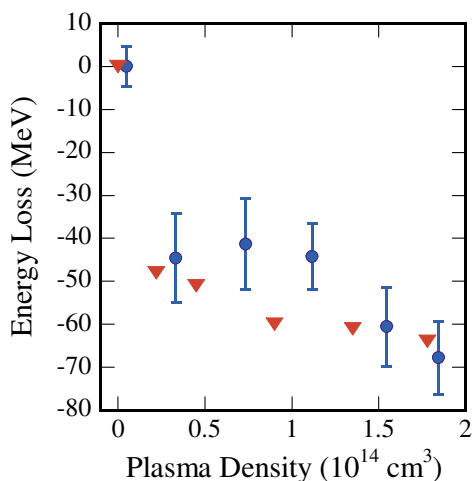


FIG. 3 (color). Energy loss of the positron beam's centroid after propagating through 1.4 m of plasma. The energy loss of the centroid increases with increasing plasma density. The red triangles are the 3D PIC simulation predictions of peak energy loss. The blue circles are the experimentally measured energy losses at different plasma densities. At a density of  $1.8 \times 10^{14} \text{ cm}^{-3}$ , the energy loss is  $68 \pm 8 \text{ MeV}$ .

Since the plasma wakefield is an energy transformer, the energy loss data strongly suggest that the particles in the beam's tail should gain energy in this experiment. As opposed to the energy loss of the beam, which can be measured at plasma densities as low as  $3 \times 10^{13} \text{ cm}^{-3}$ , the energy gain of the “tail particles” can be observed only for densities greater than  $\sim 1.5 \times 10^{14} \text{ cm}^{-3}$ . For densities less than  $1.5 \times 10^{14} \text{ cm}^{-3}$ , the plasma wakefield wavelength (see Fig. 1) is too long for the wake to accelerate enough beam charge to be measured with the limited dynamic range of the streak camera. Figure 4 shows the relative energy of each time slice along the bunch of the positron beam when the plasma is off (blue triangles) and when the plasma is turned on (red squares) with a density of  $1.8 \times 10^{14} \text{ cm}^{-3}$ . The vertical error bars represent the standard deviation of the mean for each temporal bin. Temporal resolution of the beam was possible only between the  $-4 \text{ ps}$  slice and the  $5 \text{ ps}$  slice due to the signal-to-noise ratio in the streak camera. Therefore, the first and last slices measured on the streak camera are not the true head and tail of the beam. Rather, they represent slices which lie  $\sim 2\sigma_z$  before and after the centroid. Since the change in energy is important, not the absolute energy, energy changes were measured with respect to the  $-4 \text{ ps}$  plasma off slice. The plasma off case shows that the beam has a head-to-tail energy chirp of  $\sim 20 \text{ MeV}$ . With the plasma on, energy loss is observed for the bulk of the beam out to about  $\sigma_z$  behind the centroid. The positrons behind this point have gained energy. The data show that  $\sim 5 \times 10^8$  positrons in a 1 ps slice  $1.6\sigma_z$  after the centroid were accelerated by  $79 \pm 15 \text{ MeV}$  in 1.4 m ( $\sim 56 \text{ MeV/m}$  gradient). These results are in

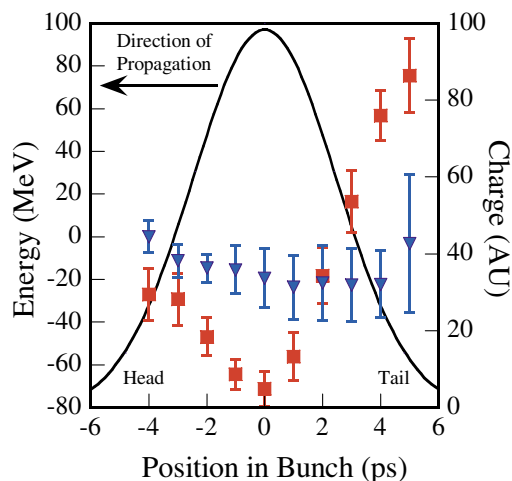


FIG. 4 (color). Time slice analysis of the energy dynamics within a single positron bunch. The plasma off (blue triangles) shows a slight head-tail energy chirp of  $\sim 20 \text{ MeV}$ . When the plasma is on (red squares), the front half of the beam loses energy driving the plasma wave, while the back half of the beam is accelerated by the plasma wave. The black line is the charge distribution within the bunch

good agreement with 3D PIC simulations which predicted a peak energy gain of 78 MeV. The maximum energy loss in the simulations occurred at about  $-1.5$  ps, whereas in the experiment the 0 ps slice (i.e., the beam's center slice) shows the greatest loss. This is thought to be due to small differences between the actual beam current profile and the fitted Gaussian current profile that was used in the simulations and also due to space-charge broadening effects in the streak camera.

In addition to the measurements in the energy-dispersive plane, the dispersion-free plane was analyzed to measure transverse dynamics of the beam's tail. One concern for energy gain measurements was that the beam's tail might have undergone transverse oscillations or hosing-type (two stream) instabilities [14] and that these oscillations would cause vertical deflections which would appear to be energy gain on our diagnostics. Our measurements of the transverse dynamics in the dispersion-free plane show no evidence of "hosing" in our data [15], thus confirming that the measurements of energy gain and loss were due to energy changes imparted on the beam by the plasma.

In summary, this Letter demonstrates the first acceleration of positrons by a plasma wakefield. Excellent agreement was found between the experimental results and those from 3D PIC simulations for both energy gain and loss. Energy loss of the centroid was found to increase with increasing plasma density up to a value of  $\approx 68$  MeV at a plasma density of  $1.8 \times 10^{14} \text{ cm}^{-3}$ . At this density, energy gain of positrons in a plasma of 79 MeV was measured. The acceleration gradient of 56 MeV/m measured in this proof-of-principal experiment can be increased to the GeV/m level in future experiments by a combination of an increase in the drive beam charge, a decrease in the drive beam pulse width (with a corresponding increase in the plasma density), and by employing a plasma channel rather than a uniform plasma [10]. Furthermore, in a real application of such a plasma wakefield accelerator, the drive positron bunch will be followed by an optimally placed trailing witness

bunch with a sufficient current to both realize high-gradient acceleration and a reasonable beam load and narrow energy spread. These scalings have been explored through PIC simulations [16]. These results and future experiments will be the basis of work to design a plasma-based linear collider which will utilize either multiple plasma wakefield accelerator sections [17] or an extremely high-gradient single stage plasma wakefield "afterburner" at the end of an existing linac to double the energy of the electron and positron beams [18].

This work is supported by U.S. DOE Grants No. DE-FG03-92ER40745, No. DE-AC03-76SF00515, No. DE-FG03-98DP00211, and No. DE-FG03-92ER40727 and by NSF Grants No. ECS-9632735, No. DMS-9722121, and NO. PHY-00787157.

- 
- [1] C. Joshi *et al.*, Phys. Plasmas **9**, 1845 (2002).
  - [2] T. Tajima and J.M. Dawson, Phys. Rev. Lett. **43**, 267 (1979).
  - [3] C. Joshi, W. Mori, T. Katsouleas, and J.M. Dawson, Nature (London) **311**, 525 (1984).
  - [4] A. Modena *et al.*, Nature (London) **377**, 606 (1995).
  - [5] D. Gordon *et al.*, Phys. Rev. Lett. **80**, 2133 (1998).
  - [6] V. Malka *et al.*, Science **298**, 1596 (2002).
  - [7] M. Everett *et al.*, Nature (London) **368**, 527 (1994).
  - [8] J.S.T. Ng *et al.*, Phys. Rev. Lett. **87**, 244801 (2001).
  - [9] M. Hogan *et al.*, Phys. Rev. Lett. **90**, 205002 (2003).
  - [10] S. Lee *et al.*, Phys. Rev. E **64**, 045501 (2001).
  - [11] R.G. Hemker *et al.*, in *Proceedings of the 1999 Particle Accelerator Conference* (IEEE, New York, 1999), Vol. 5, pp. 3672–3674.
  - [12] C. Clayton *et al.*, Phys. Rev. Lett. **88**, 154801 (2002).
  - [13] P. Muggli *et al.*, IEEE Trans. Plasma Sci. **27**, 791 (1999).
  - [14] A. Geraci and D. Whittum, Phys. Plasmas **7**, 3431 (2000).
  - [15] B. Blue *et al.* (unpublished).
  - [16] B. Blue, Ph.D. thesis, UCLA, 2003.
  - [17] J. Rosenzweig *et al.*, Nucl. Instrum. Methods Phys. Res., Sect. A **410**, 532–543 (1998).
  - [18] S. Lee *et al.*, Phys. Rev. ST Accel. Beams **5**, 011001 (2002).